Engineering Structures

Experimental and numerical analyses of rounded dovetail timber connections (RDC) under fire conditions

--Manuscript Draft--

Manuscript Number:	ENGSTRUCT_2020_1170R2
Article Type:	Research Paper
Keywords:	Timber connection; fire safety.; Rounded dovetail connection; FEM
Corresponding Author:	Rubén Regueira University of Santiago de Compostela Lugo, LUGO Spain
First Author:	Rubén Regueira
Order of Authors:	Rubén Regueira
	Juan Enrique Martinez Martinez
	Mar Alonso-Martinez
	Felipe Pedro Alvarez Rabanal
	Manuel Guaita
	Juan Jose del Coz Díaz
Manuscript Region of Origin:	Europe
Abstract:	The use of rounded dovetail connections has gained popularity in timber floor and ceiling structures due to the advance in computerized numeric control machinery. However, European building regulations for fire safety in timber structures from Eurocode 5 standard does not provide a specific method to calculate the fire performance of this kind of connections. In this work, two experimental fire tests were made to evaluate the fire performance and load-bearing capacity of this timber connection. A numerical coupled thermo-mechanical simulation of the tests was developed using the general advanced calculation methods proposed in annex B of Eurocode 5. The experimental tests showed that this connection is not able to accomplish with a R30 fire resistance class, which is the minimum requirement for lightweight timber frame assemblies. A loss of material caused by charring under the tenon of the connection leads to the failure. The general methods proposed in annex B of Eurocode 5 does not take into account the heating inside the connection. However, the simulation results showed an underestimation of the charring rate in the connection. A new simulation considering the thermal flux inside the connection was developed and it shown good agreement with the experimental tests.
Suggested Reviewers:	Salvador Ivorra sivorra@ua.es
	Javier Estévez-Cimadevila javier.estevezc@udc.es
Opposed Reviewers:	
Response to Reviewers:	

Graphical abstract

Click here to access/download;Graphical Abstract;Graphical abstract.tif

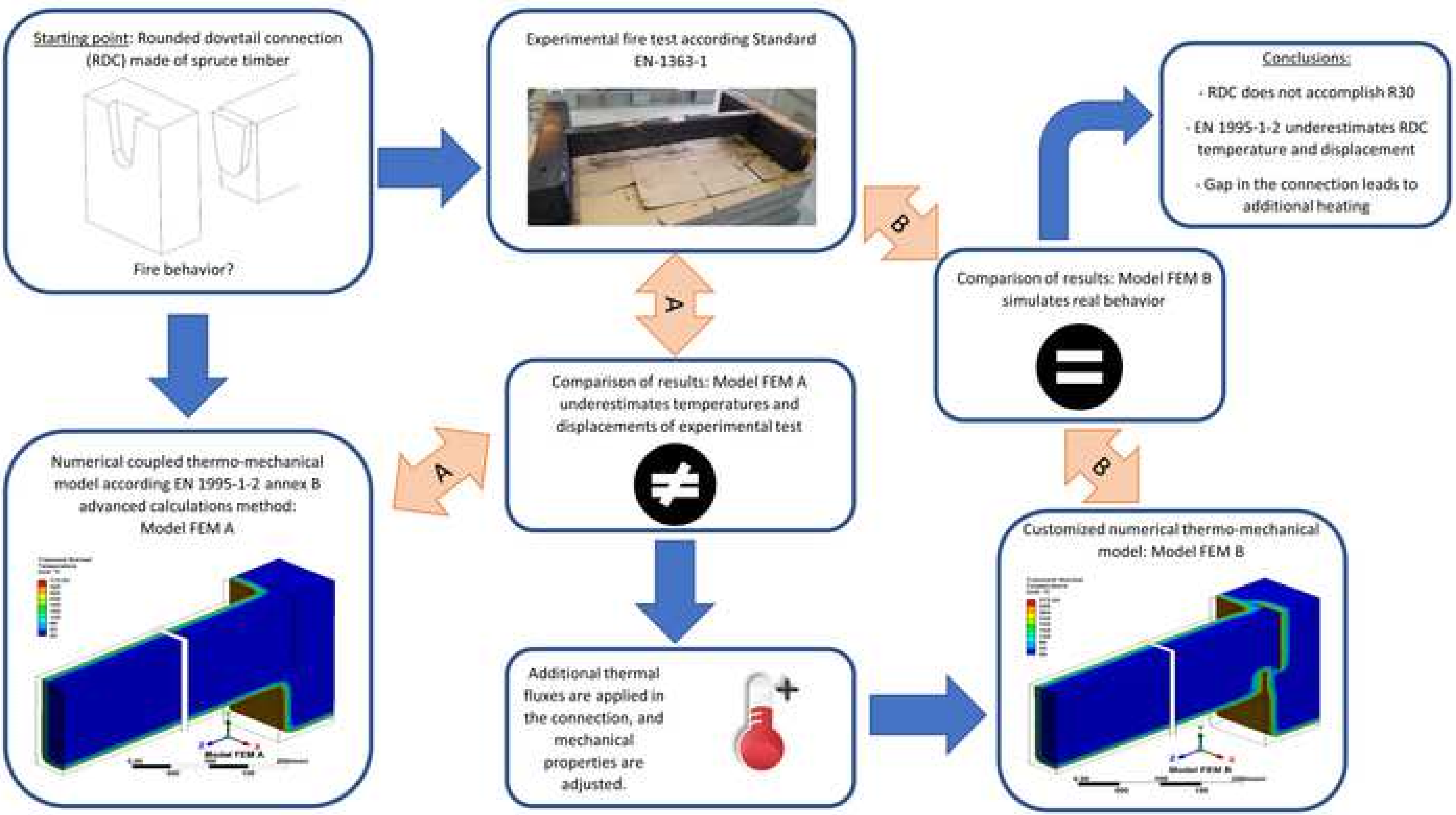

Experimental and numerical analyses of rounded dovetail timber connections (RDC) under fire conditions.

Rubén Regueira Gay[a,*], Juan Enrique Martínez-Martínez[b], Mar Alonso-Martínez[b], Felipe Pedro Álvarez Rabanal[b], Manuel Guaita Fernández[a], Juan José del Coz Díaz[b].

[a] Department of Agroforestry Engineering, University of Santiago de Compostela

[b] Department of Construction and Manufacturing Engineering, University of Oviedo

[*]: PEMADE Research Group. University of Santiago de Compostela. e-mail: ruben.regueira@usc.es (R. Regueira Gay)

Keywords: Rounded dovetail connection, Timber connection, FEM, fire safety

ABSTRACT.

The use of rounded dovetail connections has gained popularity in timber floor and ceiling structures due to the advance in computerized numeric control machinery. However, European building regulations for fire safety in timber structures from Eurocode 5 standard does not provide a specific method to calculate the fire performance of this kind of connections. In this work, two experimental fire tests were made to evaluate the fire performance and load-bearing capacity of this timber connection. A numerical coupled thermo-mechanical simulation of the tests was developed using the general advanced calculation methods proposed in annex B of Eurocode 5. The experimental tests showed that this connection is not able to accomplish with a R30 fire resistance class, which is the minimum requirement for lightweight timber frame assemblies. A loss of material caused by charring under the tenon of the connection leads to the failure. The general methods proposed in annex B of Eurocode 5 does not take into account the heating inside the connection. However, the simulation results showed an underestimation of the charring rate in the connection. A new simulation considering the thermal flux inside the connection was developed and it shown good agreement with the experimental tests.

1 Introduction

The fire performance of a timber structure is largely influenced by the behaviour of its connections [1]. The size of the cross section of a timber element decreases gradually under fire conditions. Eventually, this loss leads to the collapse of the element. The time between the ignition and the collapse of the element supporting an external load is defined as the load-bearing capacity (R) of the element [2].

The European timber construction code (Eurocode 5, part 1.2 [3]) provides methodologies to design timber connections able to withstand fire conditions. However, timber-to-timber carpentry connections are not included in this code. These connections join timber elements by cutting and fitting them, without nails, screws or bolts. The forces are transmitted from one piece to another through mortises and tenons, or notches and pins. The axial forces are transmitted through compressions and tangential forces [4].

This kind of connections were very time consuming and expensive, and consequently rarely used in building industry. In recent years, the use of carpentry connections has enjoyed a comeback due to advanced software packages and techniques to design and manufacture them. These include Computer Aided Design or Computer Aided Manufacturing (CAD/CAM) and Computer Numeric Control (CNC) [5].

The rounded dovetail connection (RDC) is a carpentry connection, particularly used in roof and floor frames. It transmits loads from secondary structural elements, such as joists, to primary structural elements such as beams. The mechanical behaviour of RDCs at ambient temperature is well known, and the critical parameters of its design have been studied [6–8]. The results show that these connections not only transfer vertical shear forces but also carry load in tension and bending. These works also show that the angle and height of the dovetail flange affect the structural behaviour of RDCs significantly. Furthermore, a probabilistic method was proposed for the improvement of RDC design. Tannert [9] conducted a series of experiments on RDC to study different methods to increase the stiffness of these structural elements. The research shows that stiffness is improved by increasing the size of the tenon or by reinforcing the joints.

Connections with dowel-type fasteners are commonly used in timber structures, and their mechanical behaviour under a fire event have been studied experimentally since the late 1970s and early 1980s [10]. In the late 1990s, fire tests on three-member timber-to-timber and steel-to-timber (with an internal steel plate) connections, and exposed to fire on all sides were performed [11–13]. These results were included in EN 1995-1-2:2004. Fire tests on other connections typologies were carried out in the 2000s by [14] and in the 2010s by [15], [16] and [17]. However, the research into the performance of carpentry-type timber connections under fire conditions is still limited. There is little work on this topic, and the one that has been made, is all about dovetail connections [18–20]. No research about any other kind of carpentry-type timber connection has been found in scientific literature. Racher et al. [18] studied dovetail connections under fire conditions. All but one of the tests exceed 15 minutes of fire exposure. Zhang et al. [19] conducted several experimental tests on straight-line dovetail joints under fire conditions. The experimental tests include protected and unprotected dovetail joints. In both cases, a gap between the tenon and the mortise was identified. The results show that the existing gap had a negligible effect on heat transfer. Furthermore, the fire-retardant coating improves the performance and significantly increases the fire protection.

These previous works do not specify the compliance with the Eurocode 5 [3] requirements for timber elements under fire conditions (R).

Experimental tests under fire conditions are extremely expensive and complicated. Numerical analysis can be used to study different geometrical joints and thermo-mechanical parameters. In this context, Regueira et al. [20] developed a finite element (FE) model to predict the mechanical performance of RDC under fire conditions. This numerical analysis, which is based on the software ANSYS, was validated using experimental results, leading to two conclusions. Firstly, the numerical results show that the temperature on the sides of the joint is influenced by its geometry. Secondly, the performance of the RDC does not meet the R30 performance criteria for fire resistance. Zhang et al. [21] developed a 3D FE model to simulate the thermo-mechanical behaviour of dovetail joints under fire conditions. The approach was validated using experimental data. The gap between the mortise and tenon is not considered in the numerical model and there is a discrepancy regarding numerical and experimental results at the beginning of tests. Despite this, there is good agreement with the experimental results.

In this research work, the load-bearing capacity of a timber beam connected to a joist using an RDC is experimentally studied under fire conditions. Then, numerical simulations using the finite element method (FEM) are developed. Firstly, two thermal models are developed using different thermal boundary conditions to study the self-protection performance of the connection. Then coupled thermal-structural models are studied and compared with the experimental results

2 Experimental study

2.1 Experimental setup

This research work studies the structural behaviour of an RDC made of common spruce timber (*Picea abies*) under fire conditions. The hygrothermal conditions of the specimens were controlled before the tests, and they had a moisture content of 13.2 % and its density had a value of 481 kg/m^3. The density was measured weighing the specimens using a scale. The beams and joists volumes were obtained measuring their dimensions using a measuring tape. The tenon and mortise volumes which were determined using CAD tools were also included adding the tenon volumes and subtracting the mortise volumes. Although the measured density is higher than the values measured in previous research works [22], it is in range with the values obtained in extended measurements [23].

Two experimental tests were conducted under fire conditions following standard ISO 834 [24] while the specimen was subjected to a sustained load. The first test studied two RDC with no fasteners and the second test studied the same geometry and included fasteners to improve the mechanical response.

The dimensions of the sample are shown in Fig. 1a. These dimensions were limited by the furnace used to carry out the experimental tests. The specimen was composed of a joist, which has a carved tenon at each end and two beams with a carved mortise in the centre to support the joist (Fig. 2). The design gap intentionally introduced between the tenon and the mortise was 3 mm. This gap increases the flexibility of the connection and facilitates the assembly of the connection.

Fig. 1. a) Dimensions of the specimen in mm. b) Specimen assembly inside the furnace.

Previous works have studied this kind of RDCs under fire conditions with no load applied [20]. This work studies the structural behaviour of the connection and the joist with a constant load applied and following ISO 834-1 fire condition [24].

Fig. 2. a) Carved mortise in the beam and b) Tenon of the RDC. (Dimensions in mm)

The specimen was placed in a custom-built furnace for intermediate-scale tests at University of Oviedo [25]. Twenty-two thermocouples were used to obtain the temperature distribution in the specimen. Eight thermocouples were placed in the centre of the joist and seven at each RDC. The thermocouples at the RDC were embedded at various depths using Type-K thermocouples, 1.5 mm in diameter. Mineral wool was used to protect all the thermocouple wires.

Thermocouples 1 to 14 were placed symmetrically at each end of the joist as shown in Fig. 3 a). Five groups of thermocouples were defined in order to measure the temperature distribution inside the connection:

- Four thermocouples (1, 7, 8, and 14) were placed inside the beam next to the mortise at a depth of 50 mm. (in red in Fig. 3)
- Four thermocouples (2, 6, 9, and 13) were placed at 36 mm from the axis of the connection at a depth of 30 mm in the external part of the tenon (in blue in Fig. 3)
- Four thermocouples (3, 5, 10, and 12) were placed at 31 mm from the axis of the connection at 80 mm in depth (in green in Fig. 3.)
- Six thermocouples (4, 11, 15, 16, 17 and 19) were placed on the longitudinal axis, at a depth of 50 mm. These thermocouples serve to compare the temperature distribution inside the joist and the beams (in black in Fig. 3.)
- Five thermocouples (18, 19, 20, 21 and 22) were placed at different distances from the joist axis, at a depth of 50 mm to study the charring rate as pyrolysis progressed from the side of the joist (in black in Fig. 3.)

Fig. 3. Placement of thermocouples in the sample: a) Top view and b) Detail views.

A constant load was applied, in the centre of the specimen, 15 min before the outset of the standard fire curve and was kept constant throughout the test. This load was set at 24 kN, which is 30% of the mean ultimate failure load of previous experimental tests at room temperature [18].

Two tests at room temperature were carried out in order to determine the ultimate loading capacity of the specimen. The procedure for the test was similar to the one described in

[26] but with just one loading point instead of two. The mean value of the ultimate load was 79.90 kN.

Experimental results

The first fire test finished after 12 minutes due to the collapse of the structure in one of the dovetail connections where thermocouples 8 to 14 were located. In the second test, the RDC are not pure carpentry connections because fasteners were added to improve the mechanical response of the connection. However, the thermal boundary conditions were the same, so thermal results are included in this work.

Fig. 4 shows the comparison between the standard fire curve (ISO 834) and the experimental curves applied in the furnace. Despite the important differences between the two curves at the beginning of the test, the standard requirements are satisfied. The Standard EN-1363-1 [27] specifies a tolerance of 15% after 300 seconds. In the first 300 seconds of the tests, there are no specifications and larger differences are accepted. The curve in the furnace was applied using three burners, see Fig. 3 a). At the beginning of the test only burner Q2 started. After 150 seconds, burners Q1 and Q3 were turned on to follow the standard curve. To understand and compare the results obtained in the test, two zones were identified as shown in Fig. 3 a): zone B, which is the area of Q2; and zone A, which is the area of Q1 and Q3.

Fig. 4. Comparison between Standard fire curve (ISO 834) and the experimental fire curves.

Fig. 5 to Fig. 8 show the temperature distribution within the structure at different positions according to Fig. 3 a). Fig. 5 shows the temperature distribution in the outside of the rounded dovetail. Two groups of temperatures were obtained. Thermocouples closer to burner Q1 and Q3 measured lower temperatures than the ones which are closer to burner Q2. This is because Q2 was started before Q1 and Q3.

Fig. 5 shows the temperature measured next to the connections between the tenon and the mortise. The temperatures obtained in thermocouples 1 and 8 are in good agreement. TC7 and TC14 measured similar values.

Fig. 5. Temperature of thermocouples 1-7-8-14.

Fig. 6 shows the thermocouples in the external part of the tenon at a depth of 30 mm. TC6 and TC13, in zone B, measured higher temperatures than TC2 and TC9, in zone A. Results show that the increase of temperature in the beam starts at 200 seconds and continues until the thermocouples reach a temperature of 100°C, when the vaporization of free water takes place. Zone B reached 100 ºC at 200 seconds and zone A at 720 seconds.

Fig. 6. Temperature of thermocouples 2-6-9-13.

Fig. 7 shows temperatures measured by TC3, TC5, TC10 and TC12. These thermocouples are located 31 mm from the axis of the connection, at a depth of 80 mm. Similar temperatures were obtained for these points. The failure of the connection in Test

1 is shown at 720 seconds in TC10 and TC12. As was seen in previous graphs, the thermocouples in zone B, TC5 and TC12, measured higher temperatures than TC3 and TC10, which are in zone A. Fig. 7 shows that there is a natural insulation which reduces the charring process.

Fig. 7. Temperature of thermocouples 3-5-10-12.

Fig. 8 shows the temperature distribution in the core of the sample. The increase of temperature measured by TC11 is related to the furnace temperature, the heat flux flowing through the gap in the connection, and the reduction of the cross-section. As the temperature increases, the charred zone grows. Therefore, the initial gap in the connection between the tenon and the beam increases, as does the heat. This effect is seen in the comparison between TC11 and TC4 after 400 seconds. The temperature at TC11, where the failure occurs, is higher than the temperature at TC4.

Fig. 8 also shows temperatures in the longitudinal axis of the joist (TC15, TC16, TC17 and TC19). Temperatures obtained in the test are very similar. TC19 is affected by the failure of the connection, so temperatures measured are slightly higher than the other thermocouples of the joist.

Fig. 8. Temperature of thermocouples 4-11-15-16-17-19.

Thermocouples 18 to 22 were placed to study the char depth. Fig. 9 shows temperature distribution in the joist from the external part to the centre. TC22 failed in the measures of Test 1 so it is negligible. The highest temperature is measured by TC22 which close to the fire exposure in zone B. TC20 measured higher temperatures than TC18 because it is in zone B where the time of fire exposure is high. TC19 measured low temperatures because is in the centre of the joist in an insulated area. However, when the failure occurs, TC19 is moved from its initial position and temperatures measured after 720 seconds are higher than expected.

Fig. 9. Temperature of thermocouples 18-19-20-21-22

The result of the sample after the fire resistance test is shown in Fig. 10. The Test 1 is finished due to the failure of one of the connections, shown in Fig. 10.a). After taking out the sample from the furnace the connection where the failure occurred was examined. A reduction of the section in the tenon and a loss of material at the bottom of the mortise were noticed.

Fig. 10. Result of fire resistance test: a) Identification of the failure connection and b) Detail of the failure in the beam and in the joist.

3 Numerical model

3.1 Finite element model

A finite element analysis (FEA) was carried out using the software ANSYS [28], which has been proved to be a valid commercial finite element software package to model timber connections under fire conditions [29]. The numerical analysis coupled a transient thermal analysis with a static structural analysis. This methodology was successfully used to simulate the behaviour of a timber connection under fire conditions [30]. In this work, the thermal performance of the timber connection is studied using two numerical models:

- model FEM A in contact without a gap between the joist and the beam;
- model FEM B with a gap and a convective heat transfer coefficient applied inside the connection.

Both numerical models are compared with the experimental results.

Symmetry conditions of the element in the longitudinal and the transverse axes are applied to simplify the numerical model. The geometry is a quarter of the joist shown in Fig. 1. A portion of the beam which supports the joist was also included in the geometry to take into account the effect of temperature on the connection.

3.1.1 Thermal model

The geometry was meshed using the element SOLID70 [28], which has 3-D thermal conduction capability. It has eight nodes with a single degree of freedom (temperature) at each node. The mesh size was set to 3 mm. using the hex dominant method. The model has 451764 nodes and 430028 elements. Fig. 11.a) shows the final result of the mesh including a detail of the mortise and tenon zone. The contact between the joist and the beam was defined as bonded using elements TARGE170 and CONTA174 [28].

Fig. 11. a) Meshing of the thermal model b) Symmetry regions and loads

The thermal properties of the material are functions of the temperature, as proposed in Annex B of Eurocode 5 [3].

The material used is *Picea abies* (spruce) with a starting bulk density of 480 kg/m^3 at 20ºC. Density decreases as temperature rises. The specific heat was defined as isotropic. It has a peak at 100ºC to consider the evaporation of the water content (moisture) inside the timber. Thermal conductivity in timber varies with the direction of the fibre. In the direction parallel to the fibre, the thermal conductivity is usually 1.8 to 2.5 times higher than in the traversal direction [31,32]. Annex B of Eurocode 5 provides the thermal properties in the transversal direction. The thermal properties in the parallel direction are increased by a multiplier coefficient of 2.0 as it was recommended in previous research works [33].

The numerical analysis was divided in 25 steps, which were carefully set to reduce convergence difficulties. The environmental temperature for each step was equal to the furnace temperature during the experimental test 1. These values are shown in Table 1

Table 1 Furnace temperatures

A convective flux and a radiative flux were applied on the fire-exposed sides of the joist and the beam. The convection coefficient (h) was 25 $W/m^2 \cdot K$ and emissivity (ε) was 0.8, as suggested by Eurocode 1 [34].

Model FEM A considers the heat transfer between the joist and the beam by conduction. However, model FEM B considers heat transfer by convection inside the gap between the joist and the beam.

Nine measured points are used in FE model to compare the evolution of temperature between the numerical model and the experimental tests. Due to the symmetry conditions of the assembly, thermocouples can be grouped as explained in section 2.1. Table 2 shows the relationship between experimental and numerical thermocouples.

Table 2 Experimental thermocouples and numerical probes equivalence

3.1.2 Coupled thermal-structural model

The geometry is a quarter of the real connection and it considers two regions of symmetry with respect to axes X and Z, see Fig. 11 a). The numerical model was meshed using SOLID186 and SOLID187 from the ANSYS element library [28]. SOLID186 is a high order 3D 20-node solid element. It has three degrees of freedom per node: translations in the nodal x, y, and z directions. The element includes heat transfer theory, so temperature may be an input nodal load or an output parameter. SOLID187 is also a high-order 3D 10-node element. It has similar capabilities to SOLID186 but is a suitable element for irregular meshes, such as the tenon zone. Temperature is also included in this element. Elements TARGE170 and CONTA174 were used to defined the nonlinear contact between the joist and the beam. The contact behaviour between the joist and the beam was defined as frictional with a friction coefficient of 0.27. It was experimentally obtained from spruce timber RDCs in previous research [35]. The mesh size was set to 10 mm, and the hex dominant method was used. The model had 9385 nodes and 1886 elements.

A constant vertical load of 6 kN was applied on a small area in the centre of the joist. This load is a quarter of the experimental load considering symmetry boundary conditions. Fixed supports are applied to the exterior sides of the beam, (see Fig. 11 b)).

The results of the thermal analysis were transferred to the structural model to consider the effect of temperature on the structural performance. Based on the experimental results, it is known that the mechanical properties of the timber change in function of the temperature. The reduction factors considered in the numerical model are shown in Table 3.

Table 3 Reduction factor for modulus of elasticity

3.2 Results

3.2.1 Thermal model

Results of the model FEM A and model FEM B thermal models are analysed separately to find differences between the two. In model FEM A, thermal loads were applied in the external faces of the joist and the beam (Fig. 12 a)). The heat transfer inside the RDC is by conduction. The temperatures obtained are lower than the experimental results. However, in model FEM B several convection boundary conditions were included inside the RDC in the tenon-mortise contact (see Fig. 12 b)). The evolution of temperature in model FEM B was similar to the experimental temperature (Fig. 17).

Fig. 12. Thermal loads applied: a) model FEM A and b) model FEM B.

Fig. 13 shows the temperature distribution in model FEM A and model FEM B after 720 seconds. The char depth is at the 300 °C isotherm, as described in [3]. The char is assumed not to contribute to the load-bearing capacity. In order to simplify the understanding of the temperature distribution, finite elements with a temperature higher than 300 ºC are not shown. In Model FEM B, the temperature reached in the beam/joist contact zone is higher than 300 °C, leading to a loss of material and a worse mechanical behaviour for the connection.

Fig. 13. Temperature map after 720 seconds. a) Model FEM A, b) Model FEM B, c) Front and side view for both models.

Fig. 14 shows the evolution of the temperatures in the virtual probes of models FEM A and FEM B in the RDC, as well as in the centre of the joist. Virtual probes in the centre of the joist are not affected by the RDC, so temperatures obtained in both models are the same. There is a slight difference in the thermal evolution of TC4 in the RDC in the two models. However, models FEM A and FEM B show noteworthy differences in the thermal behaviour of TC1, TC2 and TC3.

Fig. 14. Temperatures reached by the virtual probes: a) model FEM A in the RDC; b) model FEM B in the RDC; c) models FEM in the centre of the joist.

3.2.2 Coupled Thermal-Structural model

The main result obtained from the thermal-structural model is the deflection of the joist, see Fig. 15. In model FEM A the deflection increases linearly. However, in model FEM B, due to the boundary conditions applied, the deflection trend changes at 300 seconds. In model B at 620 seconds, there is a large vertical displacement. The evolution of deflection after the last convergence step is represented with a dotted line.

Fig. 15. Comparison of vertical displacement in the FEM models and the experimental test #1

The mechanical behaviour of the RDC is also analysed. The bearing capacity of the connection is highly dependent on the friction coefficient between the tenon and the mortise. When the load is applied, the tenon slides along the mortise and the top of the joist rotates around the beam, as shown in the static structural status in Fig. 16. The combination of sliding and rotating effects causes pressure in the connection, as shown in the static structural pressure in the mortise in Fig. 16. This behaviour was seen in previous studies [35].

Fig. 16. Mechanical behaviour of the frictional contact

4 Experimental and numerical comparison

4.1 Thermal results

4.1.1 Near the mortise-tenon zone

Fig. 17 compares the evolution of temperature in models FEM A and FEM B with the experimental results. The temperature in model A for virtual probes 1, 2 and 3 is lower than in the experimental tests. However, the evolution of temperature in model B has a similar thermal behaviour to the experimental results. Model FEM B is closer to the experimental results than FEM A.

Fig. 17. Comparison of temperatures between experimental tests and FEM models: a) TC1-7-8-14, b) TC 2-6-9-13, c) TC5-10-12 and d) TC4-11

4.1.2 The centre of the joist

The comparison between models FEM A and FEM B shows that the boundary conditions in the connection have no influence on the measured temperature in the centre of the joist. The temperatures measured by thermocouples TC18-19-20-21-22 (see Fig. 9) are higher than the numerical temperatures obtained in FE models (see Fig. 14 c)) due to the position of burner Q2. The temperature obtained in the numerical models in this zone are compared with previous research [36]. Numerical results obtained in the joist cross section are in good agreement with König tests as shown in Fig. 18.

Fig. 18. Comparison of the temperatures in the FEM model from this work and previous research from König *et al* [36]

4.2 Coupled Thermal-Structural results

The comparison between numerical models FEM A and FEM B and the experimental results considering the load applied under fire conditions are shown in Fig. 15. Until 250 seconds, the deflection obtained in the numerical models is higher than in the experimental test 1. After this, the experimental deflection measured is higher than in FEM models.

The vertical displacement obtained in the centre of the joist is smaller for the FEM A model than in FEM B model due to the thermal fluxes applied inside the mortise cavity. Model FEM B is closer to the experimental results than FEM A (see Fig. 15).

5 Conclusions

This research work presents an experimental and numerical study of the thermal-structural behaviour of timber RDC under fire conditions. Experimental results show the mechanical failure before fifteen minutes of fire exposure.

The main experimental conclusions are summarized:

- The timber RDC does not meet R30 criterion. The bearing capacity of the RDC was maintained for 720 seconds (12 minutes).
- The charring causes loss of material in the connection, which in turn causes the sliding of the RDC of the joist in the mortise (as shown in Fig. 10). This eventually leads to the failure.

The main numerical analysis conclusions are summarized:

- The thermal FE model developed following the Eurocode 5 instructions (model FEM A) obtains lower temperatures in the zone of the connection than the experimental results.
- The numerical model FEM B, with convection applied inside the connection, simulates the experimental behaviour better than model FEM A, where the heat transport is by conduction. Therefore, an important conclusion of this work is that this kind of connections are not self-protected under fire conditions.
- If thermal fluxes are applied in the inner faces of the mortise cavity (model FEM B) the coupled thermo-mechanical analysis is in good agreement with the experimental results.

The best numerical model to simulate the experimental behaviour of RDC is model FEM B where temperature distribution and mechanical response are in good agreement with experimental results. The increment of temperature inside the connection was proved due to the gap between the tenon and the mortise. Therefore, this type of connections must be carefully executed in the construction site to minimize this gap. Another solution may be to fill the gaps with fire resistant fillers.

The experimental study of timber RDC under fire conditions developed in this research work had not been previously studied in depth. Experimental results shown that RDCs are not self-protected. Furthermore, a FEM numerical model was validated with the experimental results and well-known previous research, showing good agreement.

Results of this research work suggest that timber RDCs may need fasteners to achieve load-bearing capacity (R30) following Eurocode 5. This is a direction for future work, in which it would be also interesting to consider larger and more realistic spans.

CRediT author statement

Rubén Regueira Gay: Methodology, Conceptualization, Formal analysis. Juan Enrique Martínez-Martínez: Writing - Review & Editing, Visualization. Mar Alonso-Martínez: Data curation, Writing-Original draft preparation. Felipe Pedro Álvarez Rabanal: Validation, Investigation, Resources. Manuel Guaita Fernández: Supervision. Juan José del Coz Díaz: Funding acquisition and test arrangements.

Acknowledgements

The authors of the research presented in this paper acknowledge the financial support provided by the Ministry of Science, Innovation and Universities through the National Project PGC2018-098459-B-I00 and el Gobierno del Principado de Asturias and FICYT under Research Project GRUPIN-IDI/2018/000221, both co-financed with FEDER funds. Furthermore, authors also thank the manufacturer Maderas Besteiro S.L. for the timber elements provided and finally, to Swanson Analysis Inc. for the use of ANSYS University Research program.

6 References.

[1] Frangi A, Palma P, Hugi E, Cachim P, Cruz H. Fire resistance tests on beam-to-column shear connections 2014. https://doi.org/10.3929/ETHZ-A-010189159.

[2] Science Technical Research Institute of SwedenScience Technical Research Institute of Sweden, Östman B, Winter S, Mikkola E. Fire safety in timber buildings - Technical guideline for Europe., 2010.

[3] AENOR (Asociación Española de Normalización y Certificación). Eurocode 5: Design of timber structures - Part 1-2: General - Structural fire design. 2016.

[4] Argüelles R, Arriaga F, Esteban M, Íñiguez G. Estructuras de madera. Uniones. 2015.

[5] Regueira R. Aplicación de métodos numéricos al análisis de estructuras de madera en situación de incendio. Santiago de Compostela, 2013.

[6] Tannert T. Structural performance of rounded dovetail connections. The University of British Columbia, 2008.

[7] Tannert T, Lam F, Vallée T. Structural performance of rounded dovetail connections: Experimental and numerical investigations. Eur J Wood Wood Prod 2011;69:471–82. https://doi.org/10.1007/s00107-010-0459-1.

[8] Tannert T, Haukaas T. Probabilistic models for structural performance of rounded dovetail joints. J Struct Eng (United States) 2013;139:1478–88. https://doi.org/10.1061/(ASCE)ST.1943-541X.0000744.

[9] Tannert T. Improved performance of reinforced rounded dovetail joints. Constr Build Mater 2016;118:262–7. https://doi.org/10.1016/j.conbuildmat.2016.05.038.

[10] Carling O. Fire resistance of joint details in loadbearing timber construction. A literature survey. 1989.

[11] Norén J. Load-bearing capacity of nailed joints exposed to fire. Fire Mater 1996;20:133–43.

[12] Dhima D. Vérification expérimentale de la résistance au feu des assemblages d’éléments en bois 1999.

[13] Kruppa J, Lamadon T, Racher P. Fire resistance tests of timber connections 2000.

[14] Oksanen T. Fire resistance of timber connections with stainless steel fasteners. VTT Work. Pap., 2005, p. 104.

[15] Audebert M. Approche expérimentale et modélisation du comportement au feu d’assemblages bois sous différents types de sollicitations. Université Blaise-Pascal, Clermont- Ferrand II, 2010.

[16] Werther N. Untersuchungen zum Brandverhalten von querkraftbeanspruchten Verbindungen bei Holzbaukonstruktionen, Neuentwicklung und Optimierung von Verbindungssys- temen und allgemeinen Konstruktionsregeln 2015:262.

[17] Palma P, Frangi A, Hugi E, Cachim P, Cruz H. Fire resistance tests on timber beam-to-column shear connections. J Struct Fire Eng 2016;7:41–57. https://doi.org/10.1108/JSFE-03-2016-004.

[18] Racher P, Dhima D, Audebert M, Bouchaïr A, Florence C. Fire behaviour of blind dovetail connections. 8th Int Conf Struct Fire 2014.

[19] Zhang J, Xu Y, Mei F, Li C. Experimental study on the fire performance of straight-line dovetail joints. J Wood Sci 2018;64:193–208. https://doi.org/10.1007/s10086-018-1694-z.

[20] Regueira R, Guaita M. Numerical simulation of the fire behaviour of timber dovetail connections. Fire Saf J 2018;96:1–12. https://doi.org/10.1016/j.firesaf.2017.12.005.

[21] Zhang J, Wang Y, Li L, Xu Q. Thermo-mechanical behaviour of dovetail timber joints under fire exposure. Fire Saf J 2019;107:75–88. https://doi.org/10.1016/j.firesaf.2017.11.008.

[22] Audebert M, Dhima D, Taazount M, Bouchaïr A. Thermo-mechanical behaviour of timber-to-timber connections exposed to fire. Fire Saf J 2013. https://doi.org/10.1016/j.firesaf.2013.01.007.

[23] Fischer C, Vestøl GI, Høibø O. Modelling the variability of density and bending properties of Norway spruce structural timber. Can J For Res 2016. https://doi.org/10.1139/cjfr-2016-0022.

[24] ISO 834-1. Fire-resistance tests-Elements of building construction-Part 1: General requirements 1999;1999.

[25] del Coz-Díaz JJ, Martínez-Martínez JE, Alonso-Martínez M, Álvarez Rabanal FP. Comparative study of LightWeight and Normal Concrete composite slabs behaviour under fire conditions. Eng Struct 2020;207:110196. https://doi.org/10.1016/j.engstruct.2020.110196.

[26] EN 408:2010+A1:2012 Timber structures – Structural timber and glued laminated timber – Determination of some physical and mechanical properties 2012.

[27] UNE-EN 1363-1 Ensayos de resistencia al fuego. Parte 1: Requisitos generales. 2015.

[28] Ansys® Academic Research Mechanical, Release 19.2, Mechanical User's Guide, ANSYS, Inc. n.d.

[29] Erchinger C, Frangi A, Fontana M. Fire design of steel-to-timber dowelled connections. Eng Struct 2010;32:580–9. https://doi.org/10.1016/j.engstruct.2009.11.004.

[30] Palma P. Fire behaviour of timber connections 2017. https://doi.org/10.3929/ETHZ-A-010836621.

[31] Maku T. Studies on the Heat Conductin In Wood. Bulletin 1954;13.

[32] Peter M. Numerische Tragfähigkeitsermittlung von Holzbauteilen im Brandfall unter Berücksichtigung des nichtlinearen Materialverhaltens. 2003.

[33] Erchinger C-D. Zum Verhalten von mehrschnittigen Stahl-Holz-Stabdübelverbindungen im Brandfall. IBK Bericht 2009;314. https://doi.org/10.3929/ETHZ-A-005774542.

[34] AENOR (Asociación Española de Normalización y Certificación). UNE-EN 1991-1-2. Eurocódigo 1: Acciones en estructuras. Parte 1-2: Acciones gemerales. Acciones en estructuras expuestas al fuego 2004. https://doi.org/M 23973:2004.

[35] Soilán A. Creación de modelos numéricos para el dimensionado de uniones con cola de milano entre vigas de madera estructural. Universidad de Santiago de Compostela, 2011.

[36] König J, Walleij L. One-dimensional charring of timber exposed to standard and parametric fires in initially unprotected and postprotection situations. Rapp - Traetek (Sweden) No 9908029 1999.

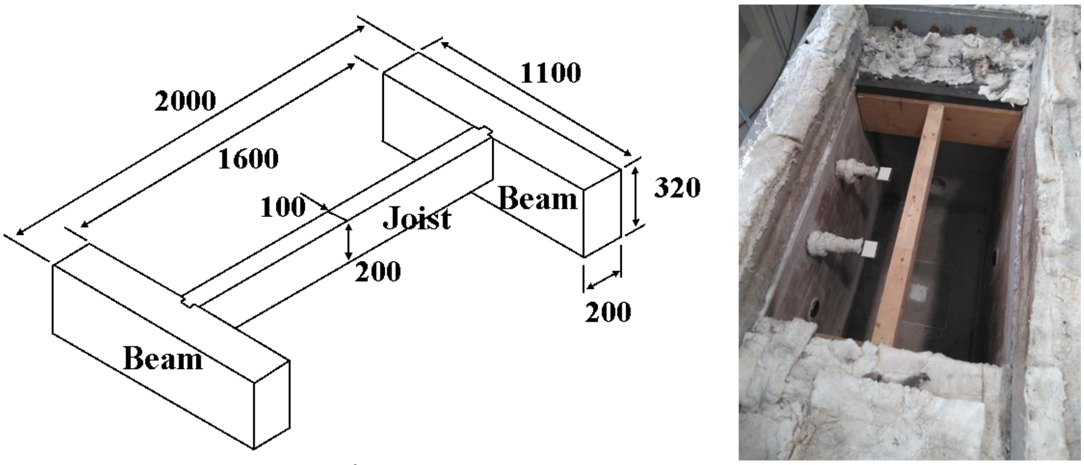

a) b)

Fig. 1. a) Dimensions of the specimen in mm. b) Specimen assembly inside the furnace.

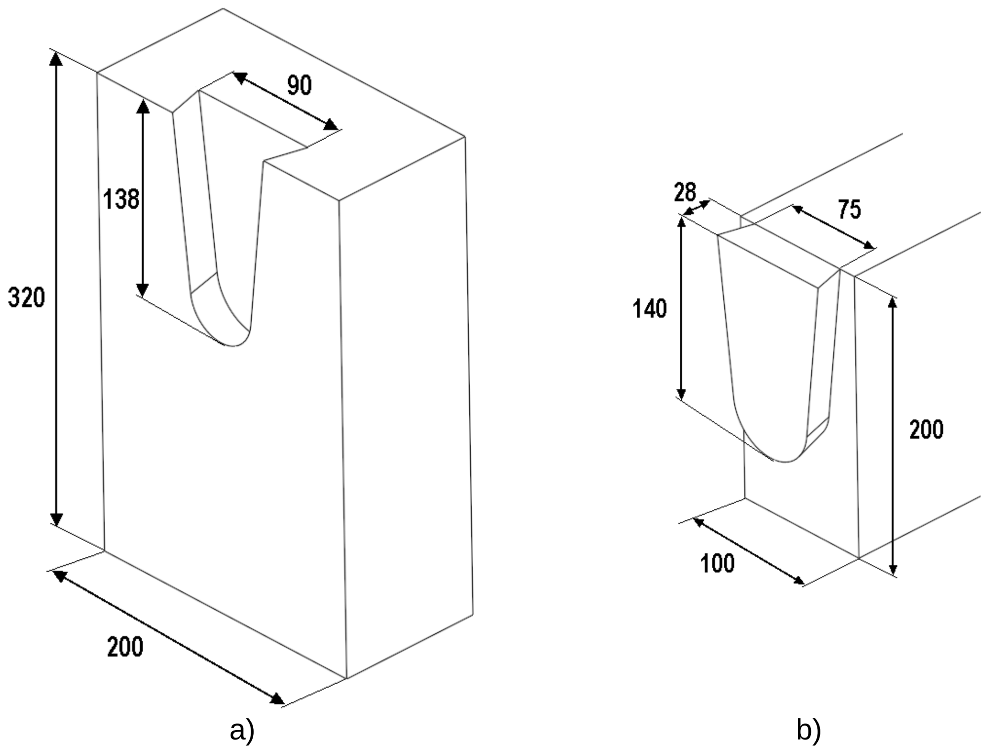

Fig. 2. a) Carved mortise in the beam and b) Tenon of the RDC. (Dimensions in mm)

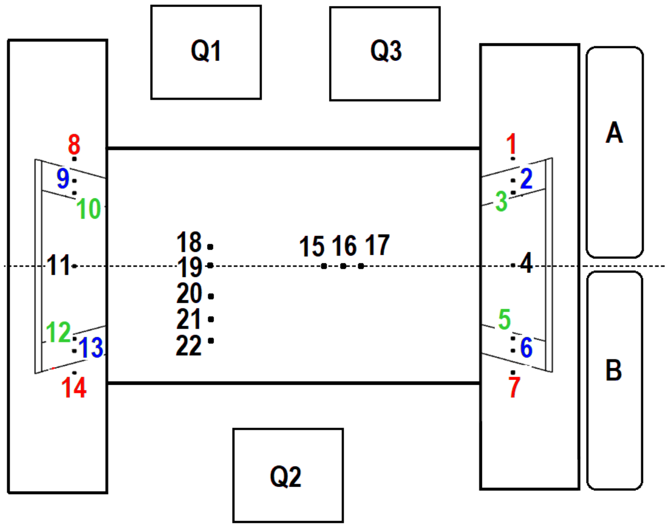

a)

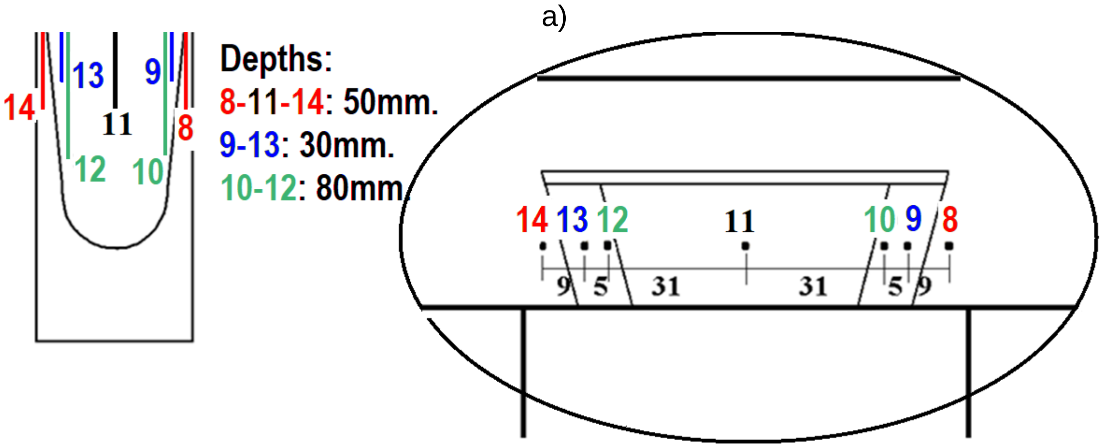

b)

Fig. 3. Placement of thermocouples in the sample: a) Top view and b) Detail views.

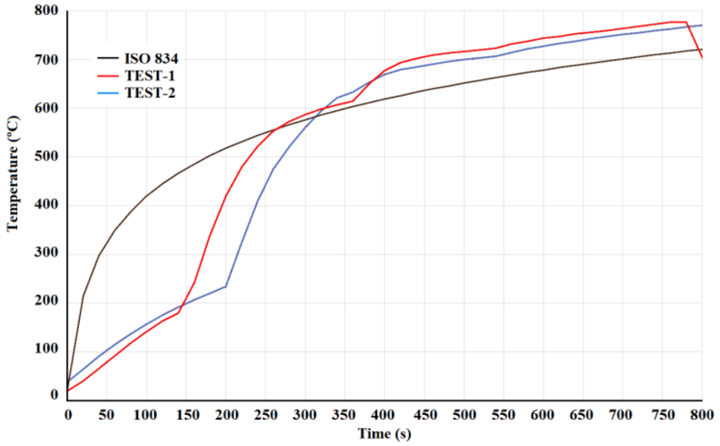

Fig. 4. Comparison between Standard fire curve (ISO 834) and the experimental fire curves.

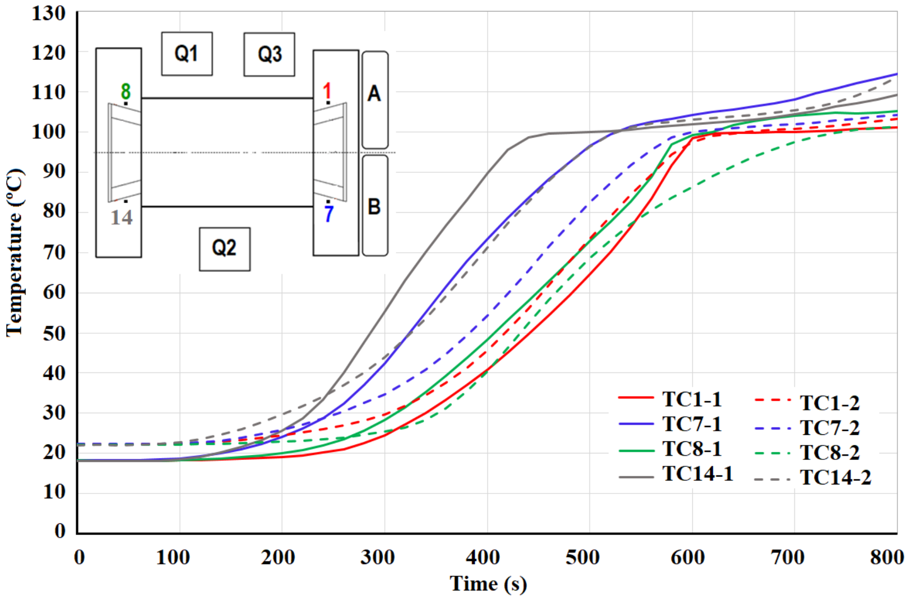

Fig. 5. Temperature of thermocouples 1-7-8-14.

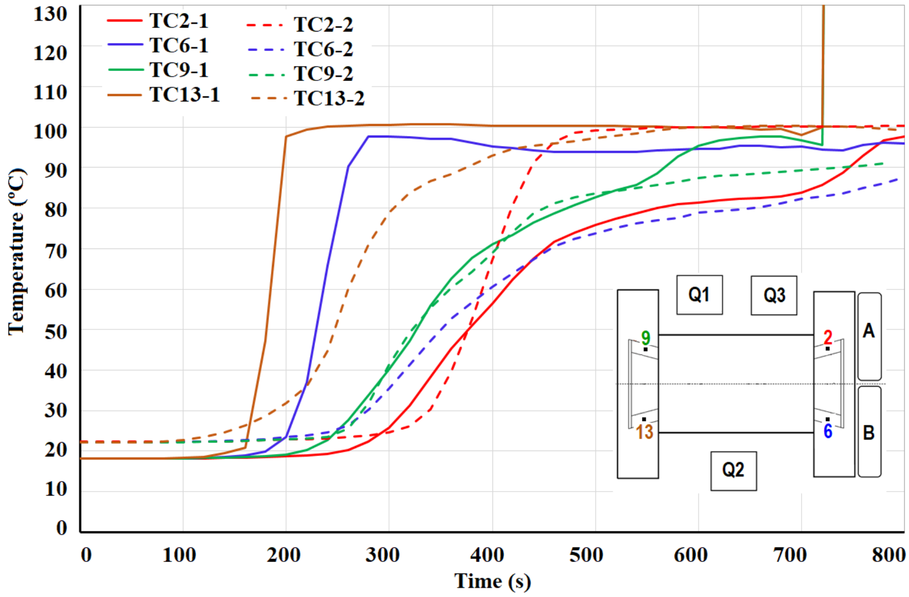

Fig. 6. Temperature of thermocouples 2-6-9-13.

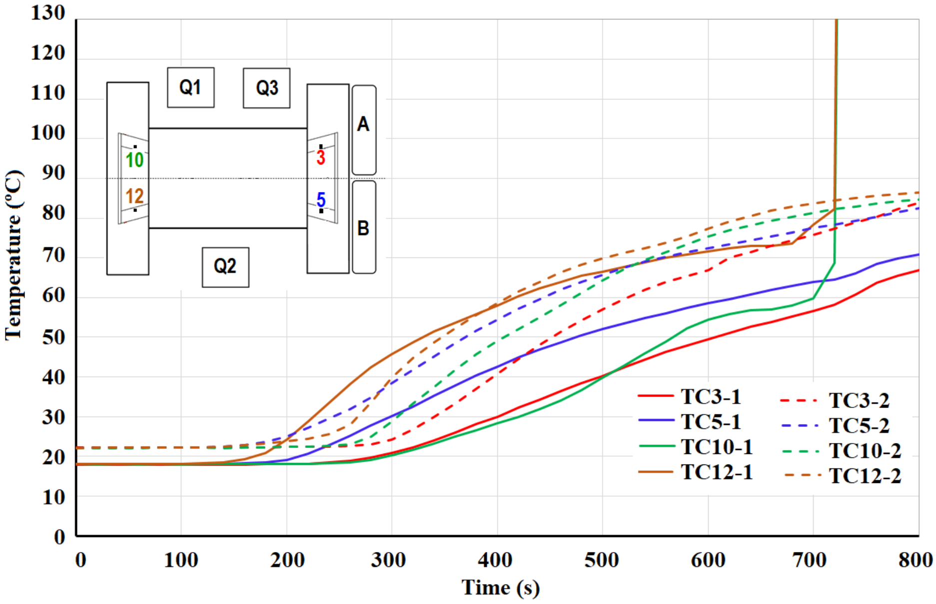

Fig. 7. Temperature of thermocouples 3-5-10-12.

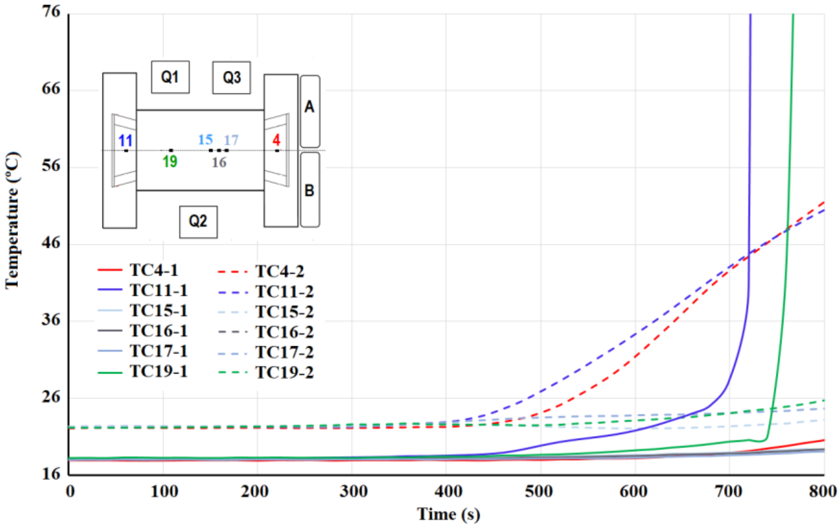

Fig. 8. Temperature of thermocouples 4-11-15-16-17-19.

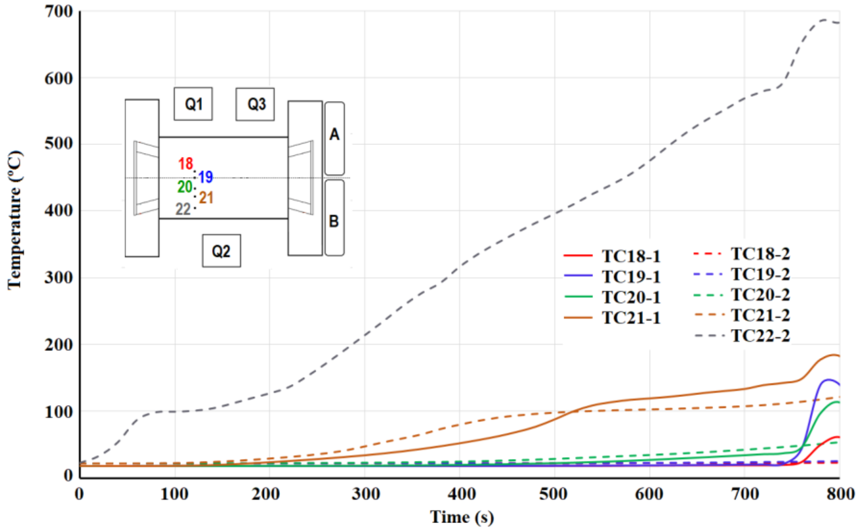

Fig. 9. Temperature of thermocouples 18-19-20-21-22

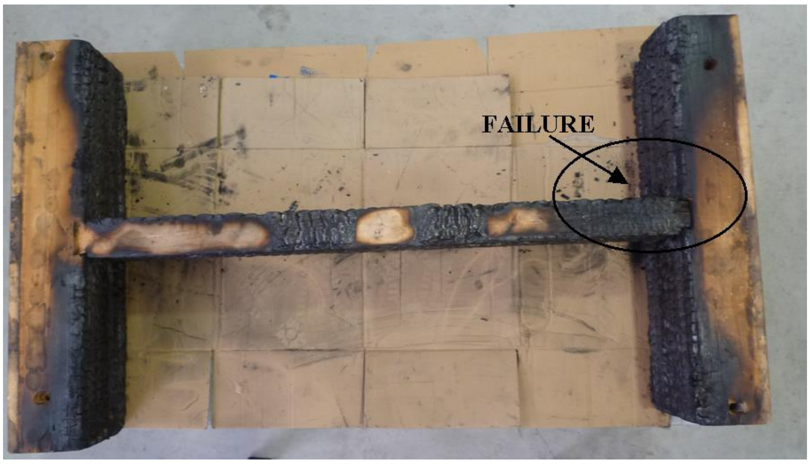

a)

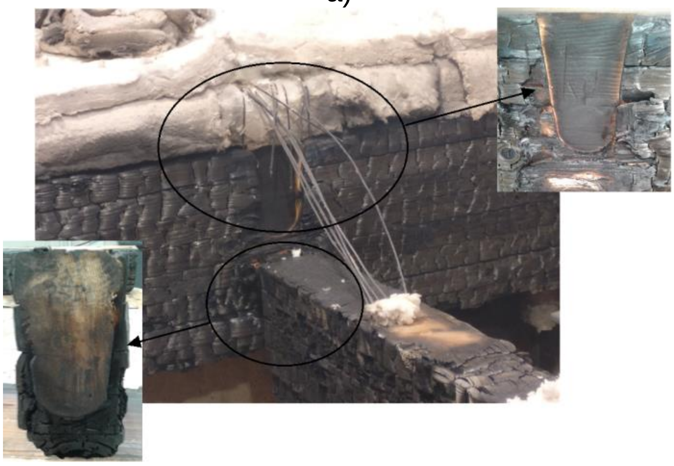

b)

Fig. 10. Result of fire resistance test: a) Identification of the failure connection and b) Detail of the failure in the beam and in the joist.

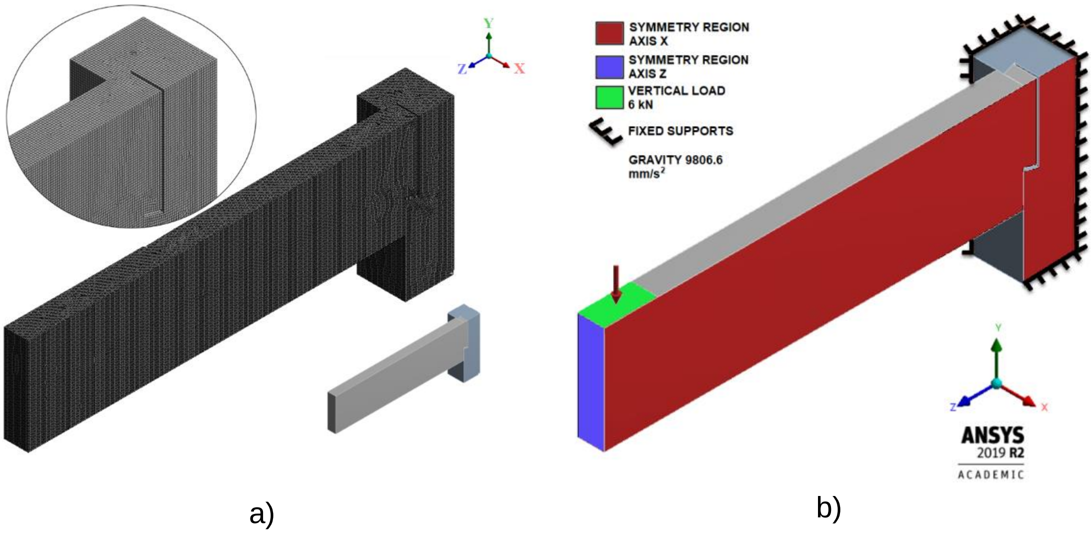

Fig. 11. a) Meshing of the thermal model b) Symmetry regions and loads

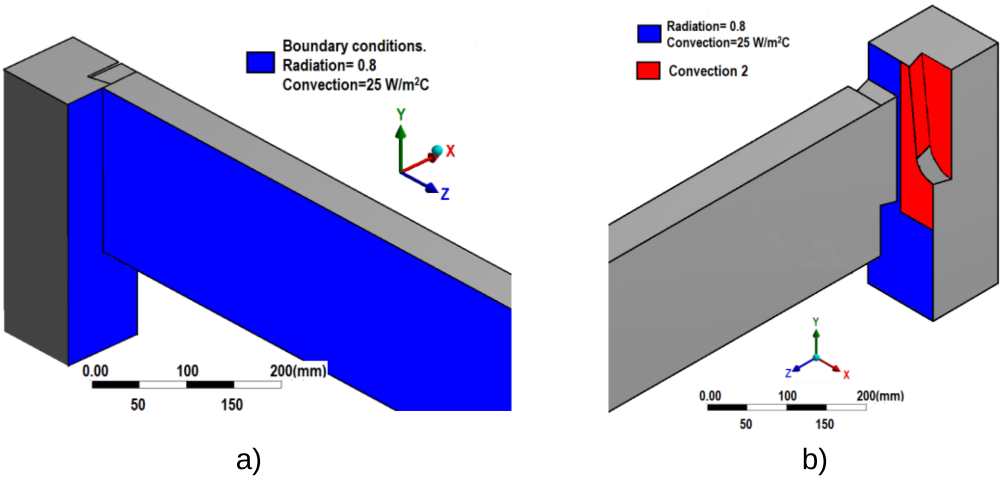

Fig. 12. Thermal loads applied: a) model FEM A and b) model FEM B.

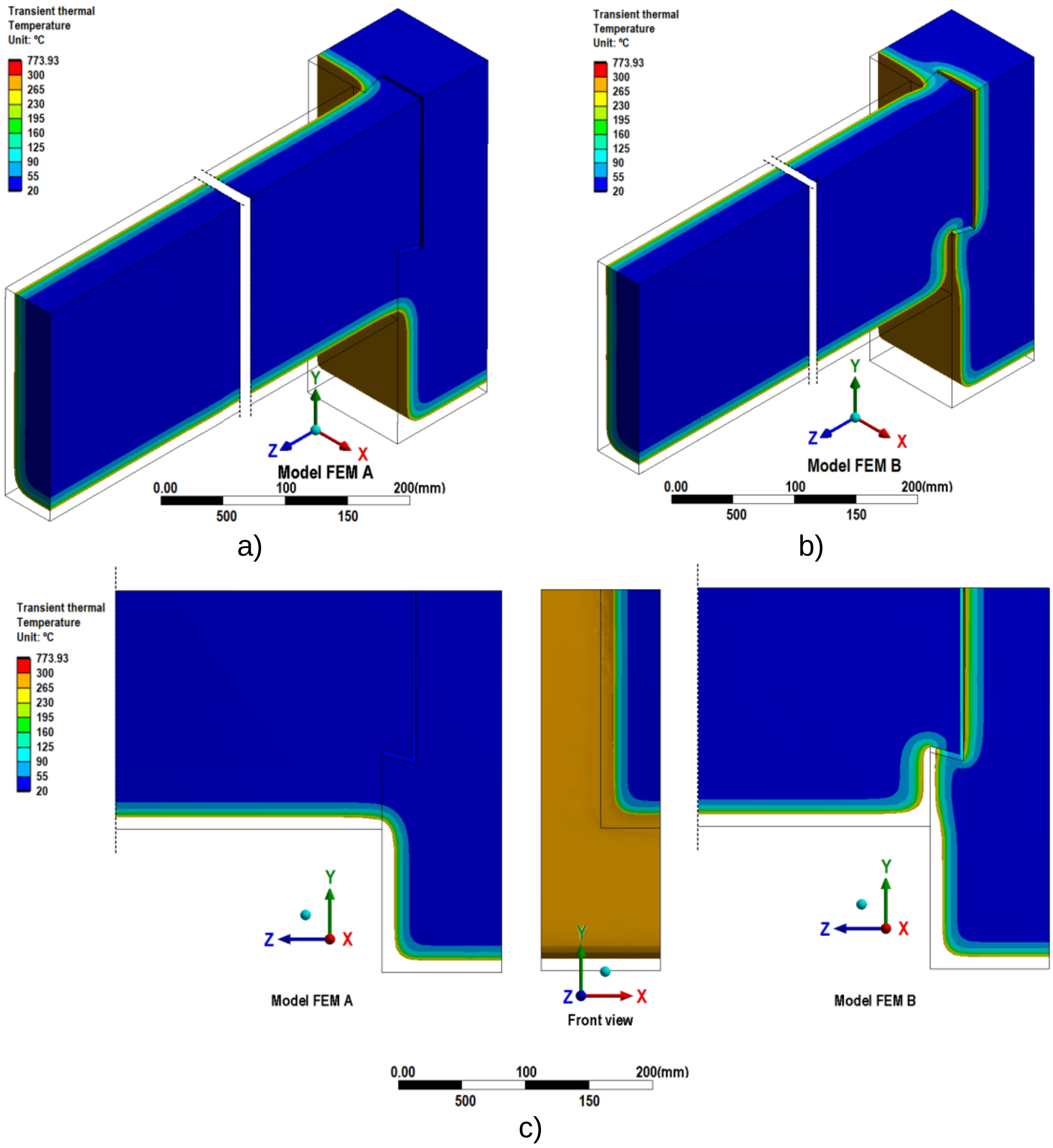

Fig. 13. Temperature map after 720 seconds. a) Model FEM A, b) Model FEM B, c) Front and side view for both models.

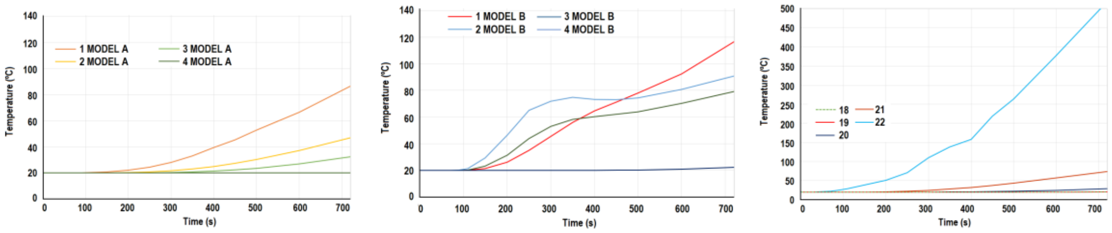

a) b) c)

Fig. 14. Temperatures reached by the virtual probes: a) model FEM A in the RDC; b) model FEM B in the RDC; c) models FEM in the centre of the joist.

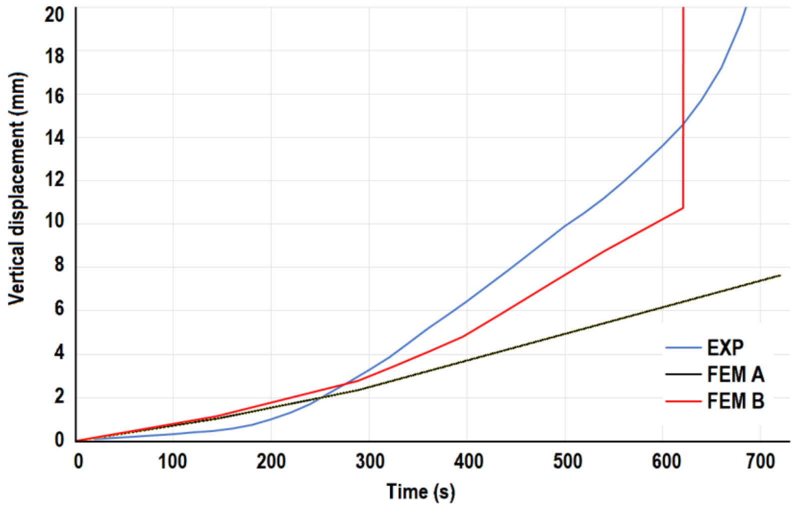

Fig. 15. Comparison of vertical displacement in the FEM models and the experimental test #1

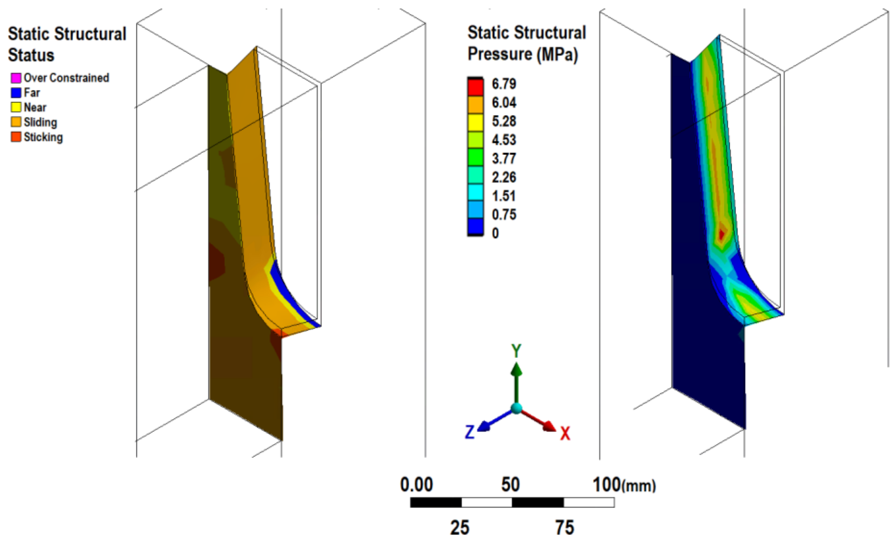

Fig. 16. Mechanical behaviour of the frictional contact

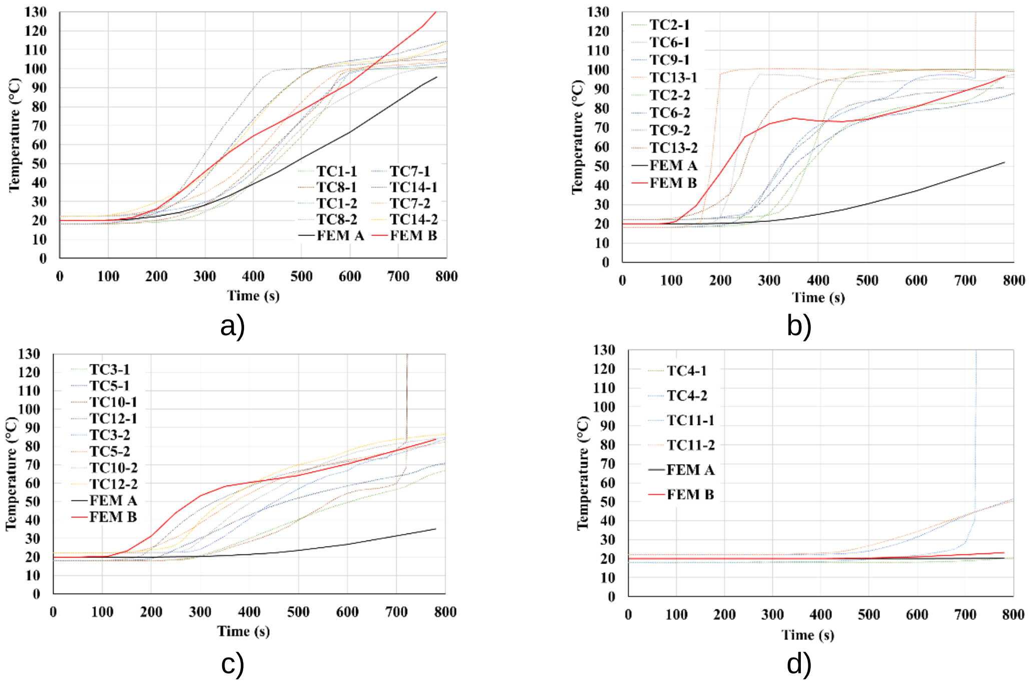

Fig. 17. Comparison of temperatures between experimental tests and FEM models: a) TC1-7-8-14, b) TC 2-6-9-13, c) TC5-10-12 and d) TC4-11

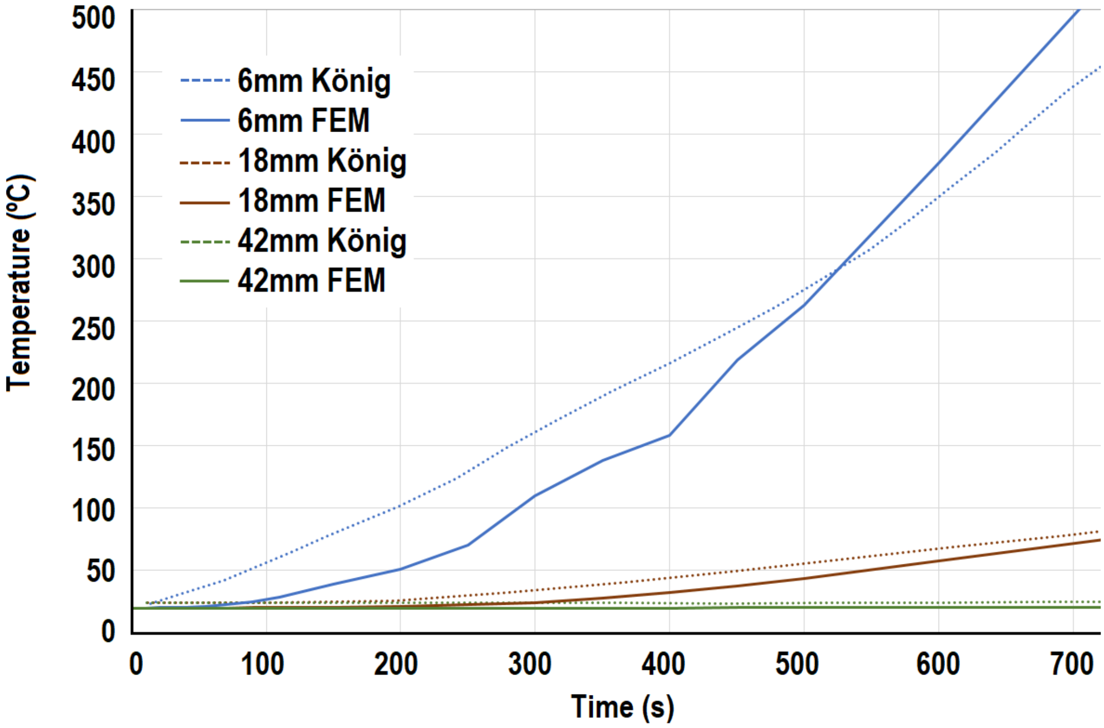

Fig. 18. Comparison of the temperatures in the FEM model from this work and previous research from König et al [34]

Tables File

Click here to access/download
Table
05_Tables.docx